IEEE Journal of Microwaves

Received 2 August 2021; revised 19 August 2021; accepted 19 August 2021. Date of publication 27 September 2021; date of current version 7 October 2021.

Digital Object Identifier 10.1109/JMW.2021.3106936

Microwaves Are Everywhere: "SMM: Nano-Microwaves"

PETER H. SIEGEL[1,2,3] (Life Fellow, IEEE)

(Special Series Paper)

[1]THz Global, La, Canada, CA 91011 USA
[2]Department of Electrical Engineering, California Institute of Technology, Pasadena, CA 91125 USA
[3]NASA Jet Propulsion Laboratory, Pasadena, CA 91109 USA (e-mail: phs@caltech.edu)

ABSTRACT If the Twentieth Century boasted of the Space Age and the Computer Age, the Twenty-First Century is certainly starting off with the Age of Biology, or at least Biochemistry. The enormous impact of CRISPR (clustered regularly interspaced short palindromic repeats), LAMP (loop-mediated isothermal amplification), cryo-EM (electron microscopy), and many other nano-techniques in the biosciences is transforming the world in so many ways, not the least of which are the diagnostic tests and vaccines that are helping our global pandemic. Microwaves are huge compared to the likes of optical wavelengths and, at least for the world of bio-spectroscopy, being able to perform and take advantage of standard microwave materials measurements at a cellular (micron) and even molecular (nanometer) scale has been a major impediment to applications for this well-developed electronics technology and instrumentation. In the early part of the 21st Century, the fields of AFM (atomic force microscopy) and SMM (scanning microwave microscopy) came together and spun off a handful of commercial applications and instruments stimulated by some very clever engineering and bio researchers and partnerships. In this, our fourth tutorial article in our continuing series on the ubiquitous presence and applications of microwaves, we take a look at the origins, instruments, biological applications, and goals for "nano-microwaves" the use of microwaves at nanometer scales.

INDEX TERMS Scanning microwave microscopy (SMM-VNA), THz near-field scattering microscopy (SMM-THz), near-field microwave imaging, near-field THz spectroscopy, nano-microwaves.

I. INTRODUCTION & HISTORICAL BACKGROUND

In the world of imaging and spectroscopy, the microwave spectrum has always provided a unique vantage point with its ability to precisely fingerprint extremely narrow band spectral signatures, and to penetrate many materials that are optically opaque. In addition, microwave sensors, which can take advantage of a vast pool of electronic circuitry and devices, have extreme sensitivity to charge distribution and movement (voltages and currents). However, when it comes to visualizing wave interactions with objects on a microscopic scale, restrictions flowing down from the late 19th century Abbe diffraction limit [1] severely constrain the smallest sample size that can be resolved to: $d = \lambda/(2n\,sin\theta)$, where d is the diameter, λ is the wavelength, n the refractive index of the medium, and θ the half angle of the focused beam on the sample. At 10 GHz, with a practical numeric aperture ($n\ sin\theta$) of 0.7, this resolution limit is approximately 2.1 cm in air and 2.6 mm in water, where n is close to 8 [2].

However, as early as 1928, self-employed Irish physicist, Edward Synge realized that much higher resolution could be obtained in principle, if the light source used to image a sample was incident through a very small sub-wavelength aperture (pinhole) in a metal film (silver deposited on a glass slide containing small granular particles to produce nm scale holes). If the sample was close enough to the metal film so that backscattered or transmitted light that "leaked" through the pin hole could be collected and focused onto a detector, a point by point image of the sample with the resolution of the pin hole could be built up [3]. Synge even came up with a piezoelectric mechanism that had sufficient resolution to scan a sample at submicron increments [4].

Unfortunately, Synge did not realize his subwavelength imaging concept, and it was not until 1972, in a remarkable (coming out of almost no prior work) three page paper in *Nature* [5] by University College of London's, Sir Eric Albert Ash[1] and George Nicholls, that Synge's ideas were demonstrated. Ash and Nichols employed an open microwave resonant cavity working at 10 GHz (λ=3 cm) above a subwavelength aperture (1.5 mm diameter), which in turn sat above, but within r_0 (the radius of the subwavelength aperture), of the sample. The sample was translated laterally, and vibrated so that a lock-in detector tuned to the vibration frequency could be used to separate out the large, scattered microwave background signal coming into the resonator and detector from the much smaller signal change induced in the resonator by the electromagnetic coupling of the near fields in the aperture to the sample itself. Ash and Nicholls correctly reasoned that the coupling through the aperture to the sample when the microwave signal was imposed from above, was via a dipole near field, and that either electric or magnetic dipole coupling to the resonator could be optimized for a particular configuration of the instrument. By raster scanning the sample under the resonator and aperture, they were able to track changes in signal level and resonant frequency sufficient to resolve a 0.5 mm grating (λ/60), λ/15 thick metal letters spelling out UCL (University College London), and to distinguish dielectric slabs with $\varepsilon_r = 2.58$ and 2.24 (Perspex and polyethylene) [5]. Finally, Ash and Nicholls pointed out that the same methods could likely be applied at optical and infrared wavelengths. For applications in the microwave bands, they suggested that their technique might be employed to measure micron-scale variations in the electric or magnetic properties of materials. The new field of **Scanning Microwave Microscopy** [2] (SMM) was born!

As with some new instrument concepts, especially those whose inventors were focused on other research opportunities (acoustics, in the case of Ash), and who did not follow up with extensive application of their new techniques themselves, it took more than 15 years before the methods demonstrated in [5] were picked up by the broader microwave community.

The optical equivalent of the Ash aperture-coupled near field microwave probe (scanning near-field optical microscopy – SNOM, or sometimes referred to as NSOM) was demonstrated, in 1984 by D.W Pohl *et al.* at IBM Zurich [8]. Pohl used a metal coated quartz fiber with a tiny hole at the tip to allow optical light inserted into the fiber to interact with an extremely close-spaced (smaller than the hole diameter) sample. Later innovators/instruments used nanometer scale metal tips simulating ultra-short dipole fields [9] as a replacement for the aperture.

The first microwave instruments to appear after the Ash and Nichols demonstration, came in the late-1980s, with an early paper from Gutmann *et al.* at RPI, Troy, NY, who utilized an aperture-coupled waveguide and a subwavelength transmission line probe [10]. In a similar diversion as Ash and Nicholls from their most referenced works, M. Fee and Steven Chu[3] at Stanford University, California, and Theodor Hänsch[4] at Max Planck Institute for Quantum Electronics in Germany, in a prescient paper in 1989 [11], coupled a commercial microwave vector network analyzer (Hewlett Packard 8510) and a now commonly employed center-conductor-extended cylindrical micro-coaxial cable probe, to scan across a sample at 2.5 GHz and achieve a resolution of 30 μm or $\approx\lambda$/4000. They also suggested a microstrip-based antenna-coupled probe design with a protruding metal tip that could be fabricated lithographically with predictable near-field coupling equivalent circuits, essential for separating out the probe parasitics from the actual sample characteristics.

Other variations of the scanning subwavelength aperture, and the conducting probe (especially the coaxial version), were realized as SMM instruments, and began to appear for localized characterization of electronic circuits and materials through the 1990s [9], [12]–[18], including operation in extreme environments, such as for characterizing superconductors [15]. Tremendous spatial resolution of $\lambda/10^7$ was achieved in the 1 MHz – 1 GHz frequency range in one of the first early tests of this concept by Keilmann, van der Weide *et al.* on a low frequency model of a coaxial transmission system as early as 1996 [9].

By 1999, the first applications of SMM in biological imaging and tissue characterization were realized, notably by Massood Tabib-Azar (now at University of Utah, Salt Lake City, USA) [19], [20]. Tabib-Azar introduced a non-contact evanescent mode probe (EMP) that used changes in the frequency and Q of a microstrip resonator in series with the probe, to obtain contrast in the sample. The instrument operated at frequencies up to 10 GHz and did not require conducting, or even solid samples [16]–[20].

[1] Sir Eric Ash (1928-) is best known for his work on acoustic microscopy. His pioneering contribution to scanning microwave microscopy is hardly mentioned in his biographies, even though it was apparently the first time the Abbe diffraction limit was signficantly superseded in a functioning microscope. The paper came out of no obvious prior published work this author could locate, and was followed up only by a few short conference papers in 1973-5 [6], [7]. However, it was both a pioneering demonstration of a completely new technique, and a major influence for the development of the scanning tunneling microscope by Gerd Binnig and Heinrich Rohr, for which they received the 1986 Nobel Prize in Physics.

[2] SMM can include widely different probe-to-sample distance ranges – those designed for nanometer scales that employ contact or very near contact probes, as in atomic force microscopy (AFM), and scanning tunneling microscopy (STM), or probes positioned further above the sample (transmission line or evanescent mode probes - EMP), typically at micron distances, but still well in the near field region. An earlier broader acronym – NSMM – for near-field scanning microwave microscopy and derived from the optical SNOM (scanning near field optical microscope) was generally employed to cover all these implementations. As NSMM became associated more and more with STM and AFM coupled probing, and SMM took on more and more electrical measurements (capacitance, current, and impedance probing) the term SMM (without the near-field designation, and imaging connotation) became popular, and was attached to the first commercial instruments. The terms are still used interchangeably.

[3] Chu later won the 1997 Nobel Prize in Physics for laser trapping of atoms and was President Barack Obama's US Secretary of Energy from 2009-2013.

[4] Hänsch won the 2005 Nobel Prize in Physics for his work on laser spectroscopy and optical frequency comb generation.

From this point forward, the possibility of using microwave signals both to characterize the electrical behavior of materials on a micro- or nano- scale, and to measure the inherent electrical properties (complex permittivity and permeability) of materials in the microwave frequency regime, including tissues and other biological samples, were now widely appreciated. Since 2000, many new variations on the original SMM themes have been presented, including scattering systems that impose the microwave signals from free space onto the probes and sample [21], comb generating input signal systems [22], extremely broadband time domain spectroscopy instruments that take advantage of short pulsed lasers or traditional broadband Fourier transform techniques in the THz regime [23], plus dozens of variations of the AFM (atomic force microscopy) and STM (scanning tunneling microscopy) probe structures to incorporate voltage, current, magnetic field, force, temperature, spin-state and charge sensing [24].

II. APPEAL OF SMM

The appeal of characterizing electronic materials (dielectrics, metals, semiconductors and even active devices) at the micron or nanometer scale, over the frequency range that these materials would be operating, is a fundamental advantage of SMM. Charge and field mapping, static and dynamic capacitance at extraordinarily small values (attoFarads:10^{-18}), spin-state, dielectric and magnetic permeability, dopant distribution, low-energy non-ionizing pump-probe measurements ideal for molecular, rather than atomic interactions, material topology and uniformity, and many other properties, have SMM signatures. There is the additional appeal of being able to characterize the microwave properties of non-electronic materials (including bio samples) on a granular scale – going down to micron or even nanometer volumes, rather than the conglomerate characterization (averaging localized variations over a large area) offered by conventional far field probing at the wavelength scale. One final characteristic that separates SMM from atomic force microscopy (AFM), and to some extent SNOM, where only the surface topography is generally mapped, is the ability of the microwave field, with its much more extensive near field power distribution volume, to penetrate below the surface of many materials and characterize, at least to some extent, the sample bulk, as well as the surface, properties.

The parallel growth of scanning near-field optical microscopy (SNOM or NSOM), as well as the widespread deployment, commercialization, and use of atomic force microscopy (AFM) and scanning tunneling microscopy (STM) instruments and techniques, helped stimulate and ultimately refine multiple arrangements for the electronic and mechanical hardware that would comprise SMM instruments as they evolved throughout the 1990s, and ultimately matured sufficiently to become a commercial product in 2007.

III. FIELD CONSIDERATIONS FOR SMM

Before considering specific SMM instrument configurations, it is helpful to review a few characteristics of the electromagnetic spectrum that are associated with moving from the macroscopic (wavelength scale) environment to the microscopic (extreme subwavelength) regime. The first involves the nature of the fields in regions close to the source (near field; distances$<<\lambda$), and many wavelengths distant from the source (far field; distances$>>\lambda$).

In the volume immediately surrounding a small subwavelength aperture or antenna excited by an RF field, the energy is typically *reactive*, confined to a region on the scale of the aperture, and can be modelled quasi-statically, that is, as a lumped element circuit – either capacitive (electric field) or inductive (magnetic field), and depends only on the physical form and dimensions of the aperture or antenna. The fields generally fall off as the square or cube of the distance (evanescent modes), and the interaction length with nearby objects is in the range of r_0, the characteristic scale of the aperture (radius) or antenna (length) [25].

If the aperture or antenna is on the scale of the excitation wavelength, the energy can be partially or fully radiative with an associated resistance and reactance, and the fields roll off approximately as the inverse of the distance. At a distance of typically $2D^2/\lambda$, where D is the aperture diameter or full antenna length, the radiating field is already a plane wave with a wave impedance ($|E|/|H|) = \sqrt{\mu/\epsilon}$, or 377 ohms in free space.

Most microwave sources, detectors, and guiding structures (coax, waveguides, striplines etc.) are optimized for this modest impedance environment between 50 and 300 ohms – represented by the free space propagation regime. When coupling microwave devices and instruments to a near field sampling system, the level of change in the scattered or reflected signals coming from the interaction of the sample with the evanescent fields at the probe tip, is extremely small compared to the power reflected from or scattered off the probe itself. Even if the aperture or short antenna is replaced by a TEM mode transmission line (as in [11]), when the conductor separation is small compared to the wavelength (in order to satisfy $r_0<<\lambda$), almost all the incident power impinging on the open end of the coax is reflected[5]. In terms of an equivalent circuit load impedance, the near field probe - whether aperture, small antenna, or open TEM line, presents an extremely large mismatch. If the exciting microwave field comes not from the confined transmission line carrying the probe, but from the free space region, and is focused onto the probe and sample, antenna reciprocity holds, and the coupling (or backscatter) of the energy in the wavelength diameter focal spot into (or from) the extreme subwavelength sized probe, will be equivalently poor (or low).

In addition, at the extremes of the quantum world (nanometer scale), samples have an inherent characteristic impedance associated with the quantum resistance ($R_Q=h/2e^2$), which comes out at approximately 12.9 kΩ [27].

[5]For example, if λ is 3 cm (frequency =10 GHz) and the source signal propagates in a Teflon filled coax cable with a core diameter of 2 mm and an inner conductor diameter of 0.6 mm (characteristic impedance Z_0 of 50 Ohms), the power reflected at the open end of the cable will be approximately 0.9988 of the incident level![26].

If the researcher is interested only in evaluating the capacitance of the sample, then this signal mismatch is not an issue, as the impedance information is contained in the reflected phase, which is easily measured by the VNA[6]. However, if complex impedance is desired, these extremely large mismatches have stimulated the use of both high Q resonators between the source and probe, as in the original Ash and Nicholls system [5], or the use of narrow band impedance transformers, to convert the probe/sample impedance to levels much closer to the characteristic impedance of the microwave feed line [28], [29], and Ch. 3 in [27]. These extra circuit elements complicate broad band measurements with SMM [30], but if not taken into account, can greatly reduce the available signal-to-noise, or lead to significant measurement errors. In fact, at least one group has reported improvements in imaging quality by removing resistive matching elements from a commercial SMM-VNA even though the mismatch was larger [31]. Moving to time domain techniques can resolve these issues [32].

IV. SMM CONFIGURATIONS

In the research community, there are almost as many variations of the SMM configuration – both electronically and at the sampling stage, as there are laboratories performing measurements. An excellent overview, despite being written two decades ago, can be found in [33]. For purposes of this short microwave-centric tutorial, we focus on only two examples. The first uses the guided wave approach of injecting microwave power into the probe through a coupled transmission line and measuring the complex reflected power (S_{11}).[7] We will refer to this configuration as the SMM-VNA, which generally works at the lower end of the microwave band. The second configuration we consider, couples broadband radiation onto the probe through free space focusing, and picks up the scattered energy in the far field. We will refer to this arrangement as the SMM-THz, since in the microwave region it has been realized mostly with THz Time Domain Spectrometer systems. SMM-THz is well suited to the 100-1000 μm band, where the wavelength and probe dimensions are slightly better matched than with the SMM-VNA, and very broad band signals are easy to generate and detect with electro-optic techniques.

In either method, the dynamic range over which one can retrieve and specify inherent material properties such as index, doping concentration, conductivity etc., depends both on the precise calibration of the instrument through a de-embedding process that separates large background signals and instrumentation or measurement errors from probe-sample coupling variations, and on an accurate equivalent circuit for the probe and surrounding near field energy, including the presence of the sample. Measurement specific calibration steps are always necessary, and especially for the SMM-THz, it can be difficult to derive absolute values for the desired sample electrical properties without calibrated references. The goal here is to briefly introduce both types of measurements and point the reader to a few commercially available systems that use similar techniques, as a guide for new researchers who may want to delve into SMM without having to become instrument designers.

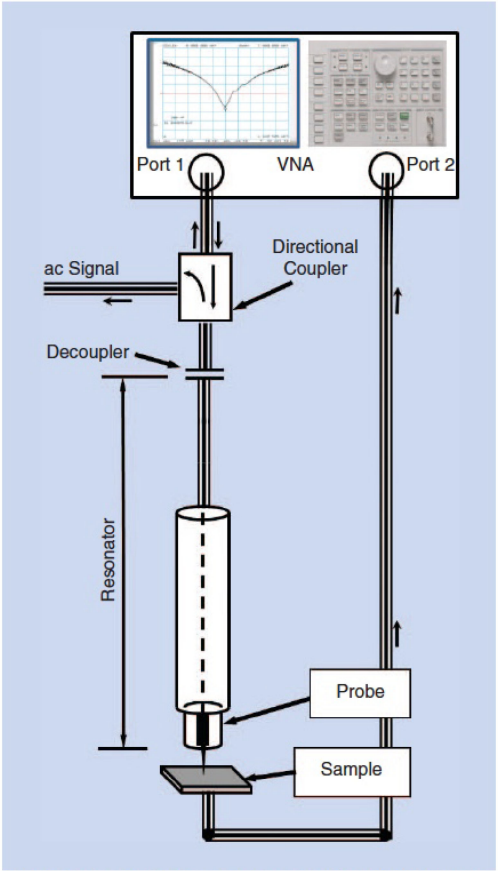

Figure 1. *The basic schematic for a typical NSMM. The resonator is coupled to the sample via a sharp probe at one end and is connected to the source and detector (VNA ports) via a decoupling capacitor at the other end. Port 1 can act as a source and a detector or alternatively can be used as a source while port 2 is used as a detector. Both detection schemes are shown in the schematic.*

FIGURE 1. Schematic of a typical SMM. From [34], ©IEEE, w/perm.

A. SMM-VNA

The SMM-VNA is based on well-developed commercial Vector Network Analyzers (S or scatter parameter analyzers) that have been in use since the 1970s. A typical configuration is shown in Figure 1, reproduced from a nice overview article on SMM [34] by the well-recognized nanoelectromagnetics team of Pavel Kabos and Thomas Wallis at NIST, Boulder, CO, USA [27]. The commercial VNA has the advantages (over a separate microwave source and detector) of producing

[6]The author thanks one of the reviewers of the manuscript for elucidating this point.

[7]It is also possible to pick up near field energy transmitted through a very thin sample and coupled to an output probe and/or detector either in close proximity or connected through a similar transmission line to a phase sensitive detector (S_{21}) [9].

a synthesized, phase coherent microwave signal sweepable over a wide frequency range, with variable source power, and complex (magnitude and phase) heterodyne detection of either reflected or transmitted signals with a very wide dynamic range (>100 dB is typical). There are also well-developed calibration techniques for removing inherent instrument errors or de-embedding sample responses from the measurement cables and sample stage.

In the depiction of Figure 1, the coaxial in-line resonator is used to convert the large mismatch at the sample plane (the end of a sharp metal tip placed within r_0 – the tip radius - of the sample) into a reactive sink (as in Ash and Nicholls original invention [5]). The resonant frequency and quality factor can be tracked with the VNA swept signal and the recording of S_{11}, the reflected power, which is at a minimum (highest sensitivity) on resonance. The sample is thus probed only at discrete frequencies of $f_r = nc/2l$, where l is the resonator electrical length, c is the speed of light and n is the mode number. For example, l might be conveniently chosen so that $\Delta f_r = c/2l = 1$ GHz. The directional coupler in the figure can be used for separating out an AC tracking signal or replaced by a bias-T to use as a DC path for current monitoring.

There are several common measurement modes involving the linear or raster scanning of the near-field probe across a sample that include: (a) measuring the resonant frequency shift and change in Q via S_{11} when the probe-to-sample platform distance is held constant and the distance to the sample surface is allowed to vary with the sample profile (enabling extraction of the profile through changes in S_{11}); (b) holding the sample surface-to-probe distance constant using a feedback loop on the vertical axis of the positioner (discussed shortly), so that changes in f_r and Q reflect differences in the sample-probe near field interaction; or (c) if the sample is conducting, recording changes in the DC or tunneling current from probe to sample at constant height above the sample, along with corresponding changes in S_{11}. The sample and probe can also have external voltage (AC or DC) applied to bias or add additional diagnostics, to particular samples. Low frequency (kHz) spatial dithering of the probe or sample by means of piezoelectric or quartz tuning elements can also be added, and monitored, through a microwave splitter and lock-in detection technique that helps separate background signals from changes at the probe-sample interface.

Although almost all commercial SMM systems (and many research devices as well) are based around commercial atomic force microscope (AFM) or scanning tunneling microscope (STM) instruments, which typically use a sharp metal tip at the end of a cantilever as the near field probe, there are a wide range of geometries that can be used. These depend heavily on the particular sample and electrical measurement being undertaken. Some of the more common RF input and probe structures are shown in Figure 2, which is reproduced from an excellent early (2007) overview of SMM techniques by Steve Anlage *et al.*, at University of Maryland [25].

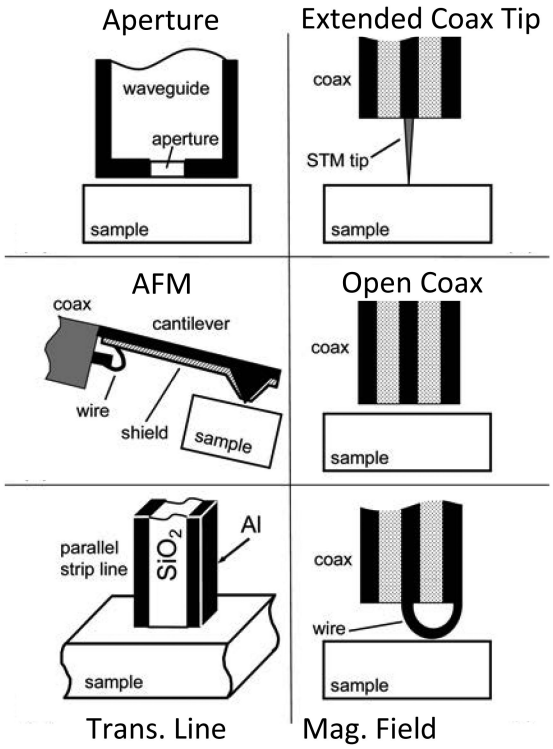

FIGURE 2. Different SMM probes. From S.M. Anlage, w/perm. A similar figure also appears in [25] with additional cross-references.

As alluded to previously, active, and tight control of the probe-to-sample distance is critical for extracting sample properties. The near-field coupling drops off at least as fast as the square of the distance, so height control at the few nm scale is essential. For the distances that many SMM instruments are designed for, the AFM/STM communities have already done an excellent job of robustly solving this positioning problem. In the case of the AFM cantilever, the very rapid change in the repulsive force that the tip undergoes when in contact with the surface of the sample is amplified and monitored through a deflection of the cantilever beam and the subsequent displacement of a reflected laser that tracks the angle of the cantilever with respect to the surface [35]. For the STM, the tunneling current amplitude (assuming the sample is conductive) is extremely sensitive to the distance of the tip above the sample and can be tracked and kept constant with an appropriate feedback loop to the vertical controller [34]. On a larger distance scale, a simple probe tip, loop, stripline, or aperture can be translated laterally (in localized sweeps) in the proximity of the sample surface, by attaching to a miniature tuning fork (crystal resonator). The resonant frequency of the cantilever or probe and crystal (generally in the kHz range) varies sufficiently with the near field coupling to the sample, to enable tracking and correcting small changes in height as the probe is scanned [36]. The tuning fork can also be mounted so as to vibrate perpendicular to the surface, and to introduce a modulation in probe height that helps decouple

variations in the near field coupling from much larger undesired background signals. In all cases, lock-in detection can be employed, as demonstrated in the original Ash and Nicholls experiments [5].

It should be noted that an SMM instrument employing an AFM or STM style probe, automatically produces all the contour parameters that a stand-alone surface profiler retrieves, in conjunction with the specific electrical and frequency dependent material (circuit) characteristics sampled by the VNA. In this way, direct maps of nanometer scale topology can be compared point-by-point to parameters such as charge distribution, capacitance, permittivity, or conductivity across a wide range of frequencies. Since the microwave fields also penetrate some distance into non-metallic samples, height-controlled sweeps, as well as frequency, can be used to interrogate material composition at different depths within the sample, a technique that separates SMM from other near field systems [37].

In order to pull out sample material properties (including penetration dependencies) from the recorded S_{11} signals or tracked changes in f_r or Q, an accurate equivalent circuit for the macroscopic VNA sampling arrangement (cabling and resonators), as well as the microscopic probe, the probe-to-sample interaction, and the sample itself, are all required. These are very measurement dependent quantities and hard to generalize. For the SMM-VNA with an AFM cantilever styled metallic probe for example, the tip-to-sample equivalent circuit is typically a small capacitance in parallel with a much larger cantilever-to-sample capacitance, which would have to be modelled or measured independently with a separate procedure, or reference standard that could be brought to bear. Similarly, for a sample from which we might want to extract the complex index or doping profile, we would have to have an equivalent circuit model for the near field coupling that could relate the measured change in f_r or Q with frequency, permittivity, and conductivity. Large sections of [25] and [27] are devoted to modelling of SMM systems and samples, and more recently, electromagnetic field solvers (finite element and finite difference time domain techniques), have become standard tools for these problems [30]. The author suspects that part of the reason there has not been more widespread use of SMM systems by researchers who are not experts in electrical engineering, is this need to accurately understand and characterize both the sample stage (probe plus holder) and the sample itself, at the measurement frequency of interest.

In addition to having a good understanding of the sample probe and SMM equivalent circuits, it is also necessary to understand and remove the inherent measurement errors associated with the VNA. Those who are familiar with modern commercial microwave analyzers know that a one port calibration (S_{11}) involves at least three measurements on three different impedance standards to remove inherent frequency dependent imperfections in various test system components, and/or to move the measurement plane from the port on the VNA to the position of the sample (de-embedding). Imperfect couplers and loads, mismatches from various connectors, losses in cabling, and other fixture related impacts on the reference and sample signal paths that are used in the VNA can be minimized, if measurements from known impedance standards implemented at the same position, and in the same environment as the sample itself, are available.

By applying a set of frequency dependent correction terms derived from measuring the supplied standards, to the imperfectly measured scattering parameters from the sample, one can significantly expand the VNA accuracy and dynamic range. Fortunately, microwave VNA's have exploited this procedure almost since their commercial introduction in the 1970s, even at the expense, the author suspects, of relaxing the performance requirements of certain critical internal components. Such tolerance errors would be calibrated out during normal measurement sequences.

For SMM, unlike the use of a wavelength scale VNA, there is no generalized method for calibrating the instrument that works with all probe-sample geometries, or even for identical probes with widely different samples. A few generalized techniques, involving capacitance and other standards [38], or stepping the height of the probe towards the sample and using predefined capacitance models to quantify observed signal changes at a specific frequency [39], [40], have proved successful for specific SMM arrangements. Time domain techniques can help with bandwidth and impedance matching [32], [41], but still tend to require standards for particular SMM arrangements and probe realizations. This is another possible hindrance to more widespread use of the SMM-VNA. The reader can revisit Ch. 8 in [27] for a much more thorough discussion.

Another calibration issue occurs as the AFM or STM tip scans across the sample and carries with it RF signal changes that are associated with the topological properties of the sample itself, which must be separated from sample electrical properties.[8] Solutions include scanning the sample stage without the sample present and subtracting point by point, or most recently, using a novel analytic method coupled to the probe geometry [42].

The SMM-VNA is a powerful technique for microscale measurements in the 0.1-100 GHz frequency regime because of the sophisticated and prevalent commercial VNA instruments that can be purchased from several vendors in the US, Europe, and Asia (e.g., USA: Keysight Technologies; Europe: Rohde & Schwarz; Asia: Anritsu Corporation). In 2007, a couple of years after acquiring Molecular Imaging Corporation from Arizona State University founders and AFM pioneers, Stuart Lindsay and Tianwei Jing [43], Agilent Technologies, Inc. announced the sale of the first large-scale commercial SMM instrument. It combined one of several slightly customized, but mostly traditional VNA's with a Molecular Imaging Corp. derived AFM and special imaging/electrical parameters software. The instrument operated from 2-20 GHz, could measure capacitance changes down to a few attoFarads,

[8]The author thanks one of the reviewers for bringing out this point and for the associated recent reference [42].

complex impedance, surface topology, and charge dopant densities [44]. It was even advertised as a biological tool for monitoring molecular interactions and ion channels [45]. It should be noted however, that the impedance transformer shown in Figure 1 was not part of the VNA and had to be custom fabricated for a particular application, and then interfaced to the standard VNA ports. Either a fixed frequency circuit with resonances every $\Delta f_r = c/2l$, or a continuously adjustable interferometric filter must be added [46], [47].

Despite an extremely loyal following, and even a major three-year European research initiative based around customizing fixtures, methods, and applications in both the semiconductor and nanobiology fields [48], Keysight (which acquired the Agilent instrument division in 2013) shut down sales and support of their SMM-VNA in 2018 [49]. According to one of the original SMM team members (paraphrasing), *"It was just one of the tools on the Swiss Army knife of AFM applications and did not have sufficient market and general application to sustain profits."* [50]. Unfortunately, this was at a time when the Keysight SMM-VNA was just beginning to show greater promise in the bio-world [51].

At least two SMM-microwave systems (no separate VNA attached) are still available: Oxford Instruments, UK who partnered with Santa Barbara's popular AFM manufacturer, Asylum Inc., in 2012, offers a whole *Swiss Army knife* of AFM tools and applications including capacitance and impedance measurements [52]. Also, PrimeNano Inc. of Santa Clara, CA, USA, which spun out of a very well established SMM research group at Stanford University led by Zhi-Xun Shen in 2013 [53], sells an enhanced resolution version of the Keysight system, boasting 0.1 attoFarad capacitance resolution and 1 nm surface resolution, but at fixed frequency (around 3 GHz) [53]. Both these instruments can give a new researcher a chance to get into the SMM-AFM world without too much of a learning curve.

B. SMM-THZ

The second type of SMM we will mention in this tutorial is based on microwave illumination of the sample together with a near field antenna, using a focused free space beam of broad bandwidth (or multiple narrow band frequencies) in order to perform direct spectroscopic measurements. A broad band receiver either picks up a small portion of the scattered energy in the far field (either back scattered or scattered in any preferred direction), or the scattered energy can be received by a second near field probe below the sample in transmission mode operation, or even as part of the probe itself [31].

The technique, sometimes called scattering scanning nearfield optical *or microwave* microscopy (s-SNOM or s-SNMM), was perfected as the atomic force microscope (AFM) became commercialized. It depends heavily on the coupling of focused source energy onto the metallic tip of the AFM, as well as the ability to modulate the tip-to-sample distance sufficiently to remove the tip from the very nonlinear region of the near field. When in close proximity to the sample, the AFM tip acts like a small dipole radiator and

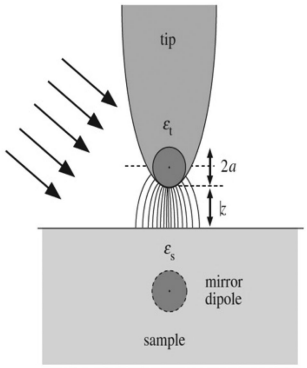

Figure 3. Modelling the near-field interaction in s-SNOM. The replacement of the probing tip by a point dipole allows to predict how the scattered light depends on (i) the distance z between tip and sample, and (ii) on the complex dielectric value ε_s of the sample.

FIGURE 3. AFM tip and sample model for a scattering SMM or SNOM. From R. Hillenbrand and F. Keilmann [62]. ©The Royal Society, UK, 2000, w/perm.

couples near field energy to the sample (Figure 3), which in turn changes the scattered far field distribution enough to be detected with a broad band receiver. The tapping (modulating) of the tip allows the near field response to be separated from the much stronger scattered signal off the other objects (pieces of the AFM and stage) within the diffraction limited signal spot.

The s-SNOM (or s-SNMM) technique was largely pioneered by Fritz Keilmann[9] , Rainer Hillenbrand, and Bernhard Knoll plus other collaborators, in the late 1990s [56]–[63] (although there were other research groups working on similar techniques, e.g. [64]–[66]). It became a commercial instrument with the founding of Neaspec GmbH, by Keilmann, Hillenbrand and Nenad Ocelic, in 2007 [67].

In the scattering-type SMM (or SNOM), like the SMM-VNA, the resolution is again limited by the tip geometry and dimensions, rather than the wavelength. $\lambda/10^3$ is typically achieved in the far infrared region [68], and much higher resolution (in terms of wavelength), has been achieved ($\lambda/10^7$) in the microwave bands [9]. At the high end of the microwave bands (THz regime) the achievable Abbe focal spot better matches the realizable AFM tip dimensions, and significantly increased coupling can be realized. Very large signal bandwidths are also possible in this frequency range using specialized THz sources that started coming online in the late 1990's (comb generators and fast THz switches operated through optical pulsed lasers). These were combined with interferometric techniques, either traditional spatially modulated FTIR (Fourier Transform InfraRed) spectroscopy using cooled bolometric detectors, or new THz time domain spectroscopy with laser-induced Auston switch style THz generation and electro-optic sampling [69], [70].

The THz regime contains a wide range of molecular signatures (weak coupling and vibrational or rotational motion) and is an important frequency region for low energy (milli-eV

[9]For a detailed technical biography of Fritz Keilmann see [55].

level) interactions. It is also an excellent frequency range for sorting out some dielectric materials that are not as readily distinguishable in the infrared or optical regions. We focus on the developmental build-up to the Neaspec commercial instrument in the following.

The idea of using an AFM style cantilever tip for a scattering SMM system goes back at least to the late 1990's when Keilmann and colleagues reported both on the techniques of focusing signals onto the tip (mostly optical and infrared) and dithering the tip vertically with respect to the sample plane to remove near-field coupling interactions from general scattering [59], [60], [61]. They also were able to accurately characterize the scattered fields from the AFM tip as arising from a short spheroidal dipole with a relative polarizability α, that depended simply on the cube of the tip radius a, and the effective complex tip dielectric constant ε_t [62]: $\alpha = 4\pi a^3 \ (\varepsilon_t - 1)/(\varepsilon_t + 2)$. This tip dipole interacts with the near-by sample through an image (mirror) dipole in the sample with polarizability $\alpha{\cdot}\beta$, where β is given by [62]: $\beta = (\varepsilon_s - 1)/(\varepsilon_s + 1)$, with ε_s the sample permittivity. Keilmann and Hillenbrand derived the effective polarizability of the tip and sample as [62]:

$\alpha_{eff} = \frac{\alpha\ (1+\beta)}{1-\alpha\beta/16\pi(\alpha+z)^3}$, with z the distance from tip to sample. Finally, since the scattered field E_s is proportional to $\alpha_{eff}E_i$, and α_{eff} can be written as a complex quantity: $\alpha_{eff} = se^{i\varphi}$, measuring relative amplitude s and the phase difference ϕ between the incident and scattered fields results in full characterization of the sample through ε_s [62]. The model as reproduced from [62], is shown in Figure 3.

In practice, both the phase and amplitude of the effective polarizability α_{eff}, only contain significant near-field interactions of the probe and the sample when the distance z, from tip to sample, is less than the radius of the tip a. Keilmann *et al.* realized that by tapping the tip from a height well beyond a ($z>>a$) all the way down to the sample surface ($z<<a$), they could modulate the near field interactions, and separate these from the much stronger signal generated by scattering off the larger objects within the focused signal spot [60]–[62]. They further found, that due to the high nonlinearity of the changes in the near field interaction at distances very close to the sample, and the fact that the tapping also partially modulated the longer distance interactions, that they had to detect at a higher modulation harmonic, typically 2 or 3, in order to get a distinctive near field signature [63] (see b. and c. in Figure 5). Note also, that in order to derive the optical constants of the sample through α_{eff}, both the magnitude and phase of the scattered energy had to be recorded. This prompted Keilmann *et al.* to use interferometric techniques in common use by both radio and optical scientists: either Fourier transform spectrometers based on movable mirrors (Michelson or Mach Zehnder implementations in particular – see Figure 4), or when they became available, stronger signal source-based time-domain spectrometers (Figure 5) that rely on THz generation through ultra-fast pulsed lasers and electro-optic switches (e.g. [69], [70]).

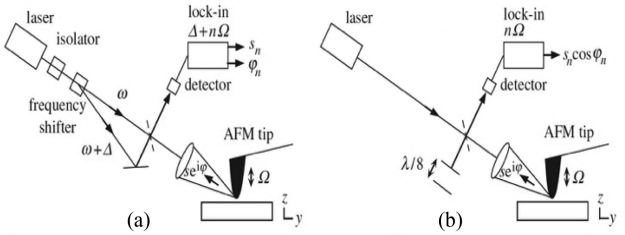

Figure 5. Sketches of optical layouts for interferometric s-SNOM. (*a*) Heterodyne system where the frequency in the reference arm of a Mach–Zehnder interferometer is offset by frequency Δ (80 MHz in Hillenbrand & Keilmann (2000)). (*b*) Homodyne system where the phase of the reference beam in a Michelson interferometer is alternated between $\psi = 0$ and 90° by mechanical mirror translation.

FIGURE 4. SMM arrangements based on scattering from an AFM tip with broadband optical energy (substitute IR or microwave) and the use of interferometric detection to collect the magnitude and phase of the scattered signals over a broad frequency band. From R. Hillenbrand and F. Keilmann [62]. ©The Royal Society, UK, 2000, w/perm.

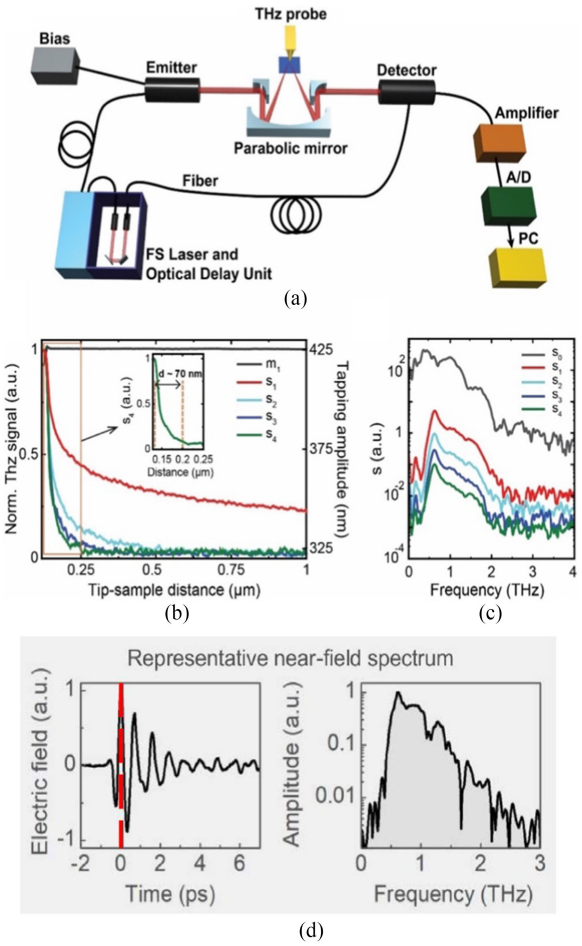

FIGURE 5. SMM-THz Time Domain Near-Field Spectrometer. (a) Schematic of THz-TDNS setup, (b) THz approach curve obtained with a commercial THz probe from Rocky Mountain Tech taken on an Au surface, (c) far-field s_0 and near-field spectra s_n obtained by detector signal demodulation of the n^{th} harmonic of the tip tapping frequency. (a)-(c) reproduced from Fig. 1 in [79], w/perm. © 2019, The Optical Society. (d) Typical time domain pulse and Fourier Transformed frequency domain spectra. From A. Huber and A. Govyadinov, Neaspec GmbH, Germany, 2021, w/perm.

The great advantage of the interferometric detection schemes, besides the ability to record magnitude and phase, was the possibility to perform measurements over an extremely wide frequency range, and hence to accomplish broad band spectroscopy on samples, while detecting extremely localized material characteristics (ε_s) that had been inaccessible beforehand [71]. Succeeding work focused on interpretation and extraction of specific material properties ([72], for example), as well as many improvements to the measurement system, including the addition of new techniques for signal illumination and detection [73]–[83]. It should be noted that Keilmann, Hillenbrand and other colleagues, all have prodigious publication portfolios involving scanning near-field techniques, but the majority of the implementations and applications fall into the infrared and optical regimes, and are not referenced here.

As mentioned earlier, the scanning SNOM system was commercialized through a spin off company, Neaspec GmbH, in 2007. Neaspec combined with Attocube Systems AG, Munich, Germany in 2014 to expand their applications. The basic THz s-SMM (scattering scanning microwave microscope) version of the Neaspec s-SNOM system is shown in Figure 5, where a THz time domain spectrometer is used as the signal source for illuminating the AFM tip. A paraboloidal mirror, that simultaneously focuses and then collects a portion of the scattered energy, is used to send the THz beam into an electro-optic detection scheme, which records the amplitude and phase of the scattered broadband THz electric fields, as the optical delay line is swept through its range (building up a time-based interferogram). A Fourier transform of the interferogram produces the spectrum in Figure 5d. (right). There are many other recent source and detector implementations, both narrow band and broadband, for the Neaspec IR and THz near-field systems, as described in [74]–[83].

As with the VNA-SMM systems, the end user has to understand a bit about the sample, and to be aware of calibration problems inherent in the topologically induced changes in the signal that the probe picks up while scanning a non-flat sample. However, because the scattering fields are so well modelled by the simple dipole interactions derived by Keilmann and colleagues, there is much less need to independently model most samples. Also, the flexibility afforded by simply focusing far-field energy onto the tip/sample, rather than having to introduce the fields through a physical cable or transmission line connected probe, make the SMM-THz suitable for many diverse applications without the need for complicated sample stages or calibration standards (although scanning both with, and without the sample present, may be necessary). Perhaps the most serious trade-off is the current lack of frequency resolution when using an interferometric technique (several GHz is typical) and determining absolute values of the sample material properties generally requires known standards to compare with. An excellent review of the scattering SMM-THz techniques by Hillenbrand and colleagues just came out in *Nature Photonics* (cover article) this past August [84].

V. SMM APPLICATIONS IN BIOLOGY

Until recently, SMM's have been mostly employed in the materials sciences and semiconductor fields. Their sensitivity to charge distribution and doping densities; index variations in compound systems; capacitance, resistivity, and conductivity; also, thermography via the conductivity; plus, permeability and superconducting properties; and bulk vs. surface properties; are all common research topics. In some instances, these applications also have remuneration potential, vis-à-vis, monitoring assembly line circuit or material fabrication processes, or the analysis of defects and faults after the fact.

As far back as the creation of the first commercial microwave tubes[10] engineering companies and medical researchers teamed up to try and take advantage of the bulk effects of this unique frequency range on biological tissues and systems [87], [88]. Early on, microwave spectroscopy was employed in many biological systems, for example, as a means to detect protein hydration as early as 1951 [89], and to distinguish chemically distinct states of oxygenated and de-oxygenated hemoglobin, as demonstrated by Keilmann in his Master's thesis in 1968 [90]. However, the cm wavelengths employed prevented any real examination of localized biological effects at, or below the cellular scale. This all changed with the advent of SMM techniques, and at least a few researchers (notably [20]), demonstrated the ability of SMM to capture information about biological substances and systems well below the Abbe diffraction limit. For an excellent, and very detailed overview, including specific calibration techniques, see Ch. 14 in [27].

The development and demonstration of a microstrip-based SMM resonant circuit and non-contacting evanescent mode probe tip [16]–[20], and subsequent integration with an AFM cantilever structure in 2002 [91], [92], by Massood Tabib-Azar then at Case Western Reserve University, Ohio, helped spur-on applications in near-field microwave microscopy for biological sampling. Tabib-Azar showed near-field images of bone and teeth at 1 GHz in 1999 [20], and in 2005, Jewook Park *et al.*, at Seoul National University, Korea, used a variation of the Tabib-Azar probe to image leaf and porcine bone tissue at 900 MHz and 1.4 GHz [93]. K. Lai *et al.* used the SMM with the AFM coaxial-style cantilever tip to image a Drosophila antenna and compound eye at 1 GHz in 2007 [94]. A similar SMM circuit arrangement, but with a patch antenna style tip, was analyzed and tested at 500 MHz on tumor shams immersed in liquids, to show imaging well below the sample surface by Reznik and Yurasova at Nizhniy Novgorod, Russia in 2005 [95]. The idea of using the SMM-VNA style techniques in biology began to catch on more strongly, and shortly after launching their commercial instrument in 2007, Agilent engineers already had in mind a major biological market [45].

[10]James Hwang points out that even as early as the use of spark gap generators there was an interest in biological applications of microwaves as in [85], [86] (personal comm., Aug 1, 2021). Synge [3], certainly had biology in mind, but for optical near-field imaging.

Meanwhile, the scattering SNOM approach (commercialized by Neaspec in 2007 [67]) was also being applied to biological samples [96]–[99], but mainly in the infrared region. At these much shorter wavelengths, established broadband interferometric spectroscopy techniques [100], and well-known water, lipid, and other protein molecular bend and stretch mode signatures, would prove to be a big advantage, once hydrated samples or full immersion liquid cells could be used.

In this context, the most recent result the author has (from Fritz Keilmann [101]), is on near field IR scanning and time sequences of living *E. Coli* and living epithelial cancer cells. To keep the organisms viable, they are immersed in prefabricated silicon holders (see Section V). Time lapse measurements can be made over hours, and movement, or even cell division can be visualized. Through their derived calibration techniques, Kaltenecker *et al.* are able to obtain full IR spectra at every point in the sample, as well as to detail and fingerprint substructures (proteins, lipids, amino acids) within the organisms [101]. Moving into the THz regime may further differentiate features within such living organisms. To the author's knowledge, these experiments have yet to be tried, although work is progressing towards this end with other THz near field instruments [102].

Returning to the SMM-VNA techniques, these began to focus heavily on biological applications about ten years ago. A group at Johannes Kepler University, Germany, and the aforementioned Agilent, Linz, team in Austria, produced detailed impedance measurements on dried human leukemia cells, both at the surface and in the bulk, from 2-10 GHz, in 2011 [103]. As already mentioned, the European Union launched a major multi-country research initiative in 2013 [48], with participation and funding from Keysight (which had just split off from Agilent). The program produced some major advances in both instrumentation and measurements for the SMM-VNA based systems, including the probing of dry cells in air [104] (Figure 6), detailed permittivity measurements on bacteria [105] (Figure 7), and new calibration techniques [38]. Keysight also began advertising the new bio-capabilities for their instrument in their application notes [106]. Most recently, the emphasis has been on ultra-fine capacitance and current measurements that can probe dipole strength and ion motion in protein membranes [107], and differences in the electron distribution in molecular assemblies at the few electrons/second (attoampere) level [108]!

Other groups were beginning to take advantage of both commercial and customized AFM-based SMM instruments, to focus on biological imaging and spectroscopy in the microwave regime. Notably, Marco Farina at Università Polytecnica delle Marche, Italy, and James C. M. Hwang at Cornell University, NY, USA. Farina and Hwang teamed up to compose a nice overview article on SMM applications in biology, which appeared last year in a special issue of IEEE MICROWAVE MAGAZINE devoted to SMM applications [109].

Almost all measurements on biological objects up to 2015, had been made with dry samples. The need to be able to probe biomaterials in their native environments (or at least in a liquid

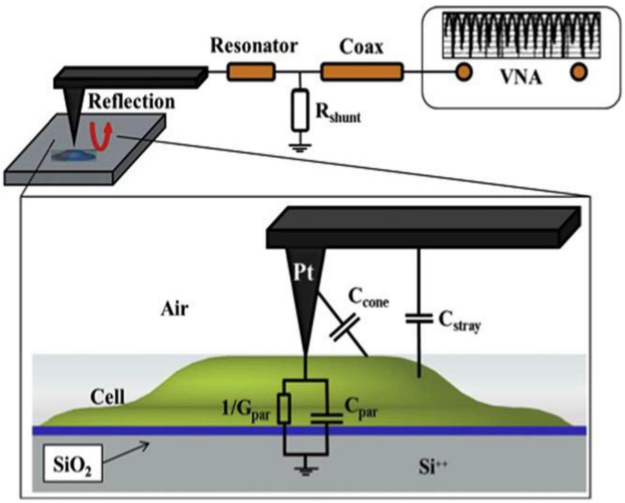

Figure 1. SMM sketch (upper panel) and equivalent electric circuit at tip/sample interaction (lower panel). SMM impedance matching network consists of half-wavelength resonator, 50 Ω shunt resistor, and coaxial cable. The lower panel presents a 3D geometrical model of a cell in contact with the fully metallic AFM probe. Equivalent electric circuit is composed of cantilever stray capacitance (C_{stray}), tip/cone capacitance (C_{cone}), and tip/sample capacitance (C_{par}) in parallel with cell conductance (loss, $1/G_{par}$). A thin layer of native SiO_2 on top of Si^{++} bulk layer forms the substrate.

FIGURE 6. SMM-VNA drawing showing set up for single cell imaging in air. Reprinted from [104], ©2016 Institute of Physics, with permission.

nutrient) where they were free to undergo respiration, move, or even divide, was clear. Farina had demonstrated a liquid immersed STM tip for SMM measurements of nanomaterials in 2012 [110]. They could then probe adhered cells immersed in open droplets or pools. In 2016, a diverse group from UC Irvine, California, USA, University of Lille, France, and University of Pennsylvania, cleverly tethered mitochondria to functionalized graphene [111], and then immersed them in nutrient fluid before probing with an SMM-VNA [112]. They even added fluorescent imaging (and tagging of the mitochondria) to monitor life signatures [113] during the scanning.

For the Farina/Hwang team, improvements in resolution, calibration, throughput, and frequency range, quickly followed their initial developments [31], [114], [115], culminating in a real time (more than 2 hour) SMM measurement sequence on living mouse myoblast cells in DMEM (nutrient solution) [116] in 2019 (Figure 8).

The same group recently introduced what they term an inverted SMM or iSMM, wherein the sample (liquid or dried) is placed on a planar slot line or coplanar waveguide which is excited by the VNA, rather than sending the signal through the AFM probe [117] (Figure 9). Now the probe acts simply as a field concentrator, and it need not be limited in design and structure by the requirement of carrying an RF signal. This has tremendous measurement advantages: it allows a full broad band 2 port measurement without the need for an impedance transformer to compensate the reflections at the end of the probe; it is less prone to background coupling from

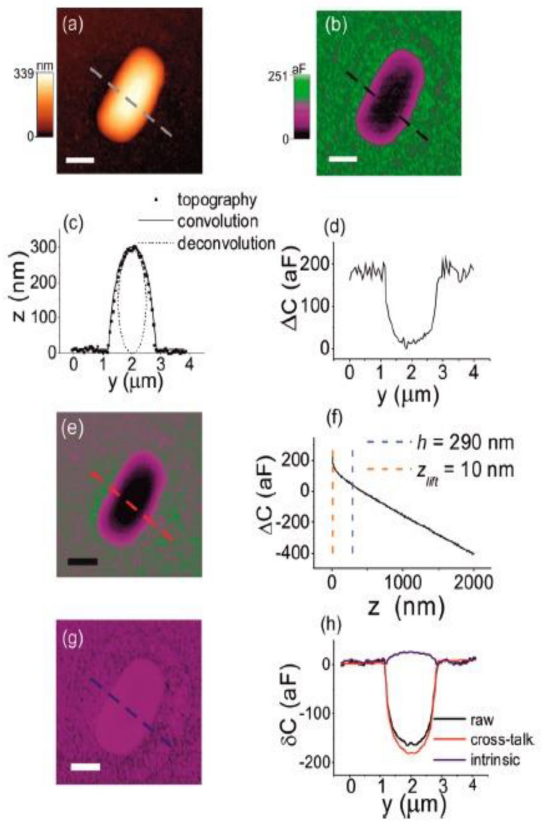

Figure 3. SMM imaging of an *E. coli* bacterial cell at ~19 GHz in dry conditions (RH ≤ 5%): (a) Topography and (b) calibrated capacitance images. (c,d) Corresponding transversal cross-section profiles along the dashed lines in the images. In (c), the actual bacterial cell cross section extracted from deconvolution of the measured topography is shown as a dotted line. (e) Reconstructed topographic cross-talk capacitance image. (f) Measured capacitance approach curve on the bare metallic substrate. The curve has been shifted by −287 aF to level it with the substrate value in the capacitance image, at the lift distance z_{lift} = 10 nm. The part of the curve used in the cross-talk reconstruction is shown between the vertical dashed lines. (g) Intrinsic capacitance image. (h) Comparison of transversal cross-sectional profiles referenced to the substrate along the dashed lines in the capacitance images in (b), (e), and (g). Scale bar 1 μm.

FIGURE 7. SMM-VNA images of E. Coli (dry). Reprinted from [105], with permission. ©2016, American Chemical Society.

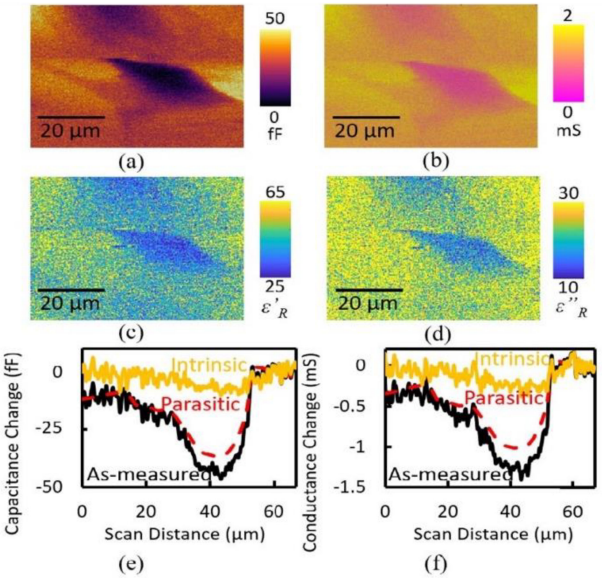

Fig. 10. Calibrated images of a live L6 cell in the D-MEM medium at 7.7 GHz by (a) capacitance, (b) conductance, (c) real relative permittivity, and (d) imaginary relative permittivity. As-measured, parasitic, and intrinsic (e) capacitance and (f) conductance for a line scan across the center of the cell.

FIGURE 8. SMM-VNA images of live mouse myoblast cell showing capacitance, conductivity, and permittivity. Reprinted from [116], with permission. ©2019, IEEE.

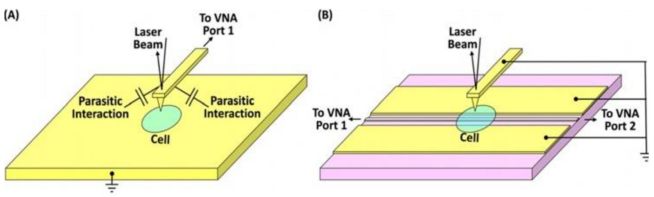

FIG. 1. Schematics of (a) a traditional AFM-modified SMM and (b) an inverted SMM. In (a), a one-port microwave measurement is performed through the AFM probe, which suffers from parasitic interaction between the probe body and the surrounding ground. The parasitic interaction is aggravated when the probe is immersed in saline solution. In (b), a two-port microwave measurement is performed through the input and output ports of a coplanar waveguide (CPW) as part of the sample holder. The parasitic interaction between the probe body and the surroundings is minimized because the probe is grounded like the grounded electrodes of the CPW.

FIGURE 9. (left) SMM-VNA using the AFM tip as the signal source and (right) the new inverted-SMM that works via a 2-port transmission line style signal path. Reprinted from [117], with permission. ©AIP Publishing, 2019.

the probe cantilever, as the probe and most of the transmission line structure around it are both grounded; and in principle the dynamic range can be dramatically improved [117]. Detailed calibration and sample isolation techniques are being developed and measurements on cells [118], as well as materials [119], have already taken place.

A last breakthrough for SMM biological sample mounting was realized when lithographically produced liquid holders became available. These were introduced by Alexander Tselev (now at Univ. Aveiro, Portugal) and colleagues at Oak Ridge National Labs, Tennessee, USA, [120] and are now commercially available. Typically, the holders consist of a silicon wafer with a central through hole, capped by a thin (10-50 nm thick) membrane (generally SiN) - Figure 10.

The holder is filled from the underside and then sealed on a glass cover slip or slide. Cells or biomaterial are allowed to sink down to the membrane where they are electrostatically or otherwise attached (they could also freely float in the solution and still be scanned, if the frequency is low, and the near field penetration extends well into the fluid). Once the cells adhere, the holder is flipped and ready to scan. The AFM probing is

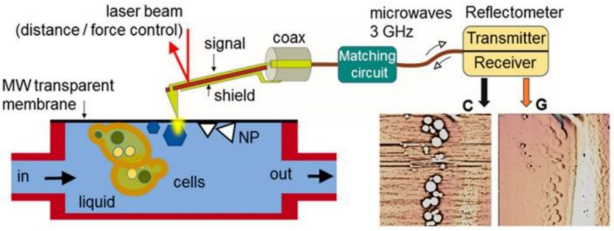

Figure 1. Layout of the experimental setup for near-field scanning microwave impedance microscopy in liquids. An AFM-type scanning probe is integrated into an AFM setup for probe scanning over the sample surface with control of the probe–sample distance and force. In addition to the sample topography, two more channels-capacitance C and conductance G-are used for mapping and imaging. The capacitance and conductance of the tip–sample system are monitored by a microwave reflectometer operating at a frequency of 3 GHz. The objects under study are enclosed in a capsule filled with a fluid (or gas) and separated from the probe by an ultrathin dielectric membrane transparent for microwave radiation.

FIGURE 10. Depiction of a liquid biological sample cell with SMM probing from above using an AFM tip through a thin transparent membrane. Reprinted from [120], with permission. ©2016, American Chemical Society.

then accomplished directly through the membrane, with penetration into the liquid or immersed cells. This technique has just been employed extremely successfully with an infrared scattering type s-SNOM to probe living *E. Coli* [101]. One can imagine improving the technique further by coupling to microfluidics and/or functionalizing the membrane for better, or more specific biomaterial adhesion. Tselev describes the invention, detailed implementation, use and characterization of these holders in the aforementioned special issue of IEEE MICROWAVE MAGAZINE [121].

VI. SUMMARY

Biological probing of cells, organelles, proteins, or even individual molecules at microwave frequencies has just begun to establish an observable presence in biology and electrochemistry. The last five years have witnessed a dramatic improvement in SMM capability, calibration, and modelling, to better derive absolute sample material characteristics. Scanners can now accommodate hydrated and fully immersed living organisms, which can be measured or probed without direct contact and without significant energy transfer from the probe. SMM instruments have also diversified and been focused directly on a range of specific properties: capacitance variation, impedance measurements, dielectric spectroscopy, current or ion probing, and many other tools that constitute the plethora of AFM and STM based techniques (new acronyms often emerge well before any real physical merits have been demonstrated). Although there are only a handful of highly active research groups, and just a couple of commercial suppliers of SMM instruments and accessories, progress towards more standardized and accommodating probing circuits and sampling arrangements is progressing. Hopefully, these will begin to evolve into more turnkey systems in the not-too-distant future.

At this time there does not seem to be a particular SMM signature that is so critical to the biological or biochemical communities that would establish SMM as a central and ubiquitous tool. However, the potential for untagged biochemical fingerprinting, following ions through membranes, and charge distributions at the scale and quantity relevant to just a handful of individual molecules, plus quantifying the electrical properties of subcellular organelles and small groups of proteins, all seem to be within reach.

Although many of the nanometer-scale microwave permittivity measurements to date, on both wet and dry samples, seem to correlate well with macroscopic values, the author leaves off with an interesting paper that was recently pointed out to him by Fritz Keilmann. In 2018, an AFM style probe was used with a scanning dielectric microscope to measure extremely thin (3-6 Å) confined water films (surface layers inside very thin channels) and it was found that the dielectric constant of these surface layers was not 80 – the normal bulk value for water, *but only 2.1* [122]. The explanation, according to the authors, is consistent with the complete suppression of dipole rotational motion! The bulk water index value was not reached until the film thickness was close to 100 nm. The implications for biochemistry are intriguing, and SMM techniques seem to be an ideal way to probe these types of nanoscale molecular characteristics and interactions.

From the Universe [123] to the "nanoverse", ***Microwaves are Everywhere!***

ACKNOWLEGEMENTS

The author would like to thank Ferry Kienberger from Keysight Linz, Austria, and Georg Gramse from Johannes Kepler University (and Keysight), Linz, Austria, for their extremely helpful information on the commercial SMM-VNA system, and their excellent references (and incredible technical accomplishments in SMM). Also, for permission to reprint Figures 6 and 7. Similarly he would like to thank Andreas Huber and Alexander Govyadinov, at Neaspec GmbH, Martinsried, Germany, for information on the SMM-THz system, some useful references, and for Figure 5 used in the text. The author is also extremely grateful for the correspondence with Rainer Hillenbrand at CIC NanoGUNE in San Sebastian, Spain, and for his very helpful references and suggestions on THz s-SNOM techniques. A very special thank you is due to long-time colleague and friend, Fritz Keilmann, at Ludwig Maximilian University of Munich, Germany, for several references, his recent preprint, the article on the dielectric measurement of water surfaces, and permission for reuse of Figures 3 and 4. Skip Young, Michael Slayton and Jeff Neal of Keysight USA, and Song Xu, of Nanocue Technology, West Bloomfield, MI, USA, provided some additional details and contacts for their commercial SMM-VNA instrument. Steve Anlage at University of Maryland, College Park, James C. M. Hwang at Cornell University, Ithaca, NY, Pavel Kabos at NIST, Boulder, Colorado, USA, and Alex Tselev at University of Aveiro, Portugal, were all extremely helpful in supplying references, advice, and figure reprint permissions (Figure 1 – Kabos, Figure 2 – Anlage, Figures 8 and 9 – Hwang, Figure 10

- Tselev). Finally, the author is extremely grateful to Fritz Keilmann and Jim Hwang for reading over relevant sections of the paper for accuracy and for comments, and to one of the reviewers for elucidating and suggesting fixes for several misconceptions in the original text.

REFERENCES

[1] E. Abbe, "VIII. The relation of aperture and power in the microscope," *J. Roy. Microscopical Soc.,* London, U.K., pp. 300–309, 1882; plus "XI. The relation of aperture and power in the microscope, (continued)," *J. Roy. Microscopical Soc.*, London, U.K., pp. 460-473, 1882, plus "XV. The relation of aperture and power in the microscope, (continued)," *J. Roy. Microscopical Soc.*, London, U.K., pp. 790-812, 1883.

[2] U. Kaatze, "Complex permittivity of water as a function of frequency and temperature," *J. Chem. Eng. Data*, vol. 34, pp. 371–374, 1989.

[3] E. H. Synge, "XXXVIII. A suggested method for extending the microscopic resolution into the ultramicroscopic region," *London, Edinburgh, Dublin Philos. Mag. J. Sci.*, vol. 6, no. 35, pp. 356–362, 1928.

[4] E. H. Synge, "XXIII. An application of piezo-electricity to microscopy," *London, Edinburgh, Dublin Philos. Mag. J. Sci.*, vol. 13, no. 83, pp. 297–300, 1931.

[5] E. A. Ash and G. Nicholls, "Super-resolution aperture scanning microscope," *Nature*, vol. 237, no. 5357, pp. 510–512, 1972.

[6] E. A. Ash and A. Husain, "Surface examination using a superresolution scanning microwave microscope," in *Proc. 3rd Eur. Microw. Conf.*, 1973, pp. 1–4.

[7] A. Husain and E. A. Ash, "Microwave scanning microscopy for non-destructive testing," in *Proc. 5th Eur. Microw. Conf.*, 1975, pp. 213–217.

[8] D. W. Pohl, W. Denk, and M. Lanz, "Optical stethoscopy: Image recording with resolution λ/20," *Appl. Phys. Lett.*, vol. 44, no. 7, pp. 651–653, 1984.

[9] F. Keilmann, D. W. van der Weide, T. Eickelkamp, R. Merz, and D. Stöckle, "Extreme sub-wavelength resolution with a scanning radio-frequency transmission microscope," *Opt. Commun.*, vol. 129, no. 1/2, pp. 15–18, 1996.

[10] R. J. Gutmann, J. M. Borrego, P. Chakrabarti, and M.-S. Wang, "Microwave scanning microscopy for planar structure diagnostics," in *IEEE MTT-S Int. Microw. Symp. Dig.*, 1987, pp. 281–284.

[11] M. Fee, S. Chu, and T. W. Hänsch, "Scanning electromagnetic transmission line microscope with sub-wavelength resolution," *Opt. Commun*., vol. 69, no. 3/4, pp. 219–224, 1989.

[12] C. Bohm, C. Roths, and E. Kubalek, "Contactless electrical characterization of MMICs by device internal electrical sampling scanning-force-microscopy," in *IEEE MTT-S Int. Microw. Symp. Dig.*, vol. 3, pp. 1605–1608, 1994.

[13] T. Wei, X. D. Xiang, W. G. Wallace-Freedman, and P. G. Schultz, "Scanning tip microwave near-field microscope," *Appl. Phys. Lett.*, vol. 68, no. 24, pp. 3506–3508, 1996.

[14] C. P. Vlahacos, R. C. Black, S. M. Anlage, A. Amar, and F. C. Wellstood, "Near-field scanning microwave microscope with 100 μm resolution," *Appl. Phys. Lett.,* vol. 69, no. 21, pp. 3272–3274, 1996.

[15] S. M. Anlage, C. P. Vlahacos, S. Dutta, and F. C. Wellstood, "Scanning microwave microscopy of active superconducting microwave devices," *IEEE. Trans. Appl. Supercond.*, vol. 7, no. 2, pp. 3686–3689, Jun. 1997.

[16] M. Tabib-Azar, N. S. Shoemaker, and S. Harris, "Non-destructive characterization of materials by evanescent microwaves," *Meas. Sci. Technol.*, vol. 4, pp. 583–590, 1993.

[17] M. Tabib-Azar, D.-P. Su, A. Pohar, S. R. LeClair, and G. Ponchak, "0.4 μm spatial resolution with 1 GHz (l = 30 cm) evanescent microwave probe," *Rev. Sci. Instrum.,* vol. 70, no. 3, pp. 1725–1729, 1999.

[18] M. Tabib-Azar, P. S. Pathak, G. Ponchak, and S. R. LeClair, "Nondestructive super resolution imaging of defects and nonuniformities in metals, semiconductors, dielectrics, composites, and plants using evanescent microwaves," *Rev. Sci. Instrum.*, vol. 70, no. 6, pp. 2783–2792, 1999.

[19] M. Tabib-Azar, R. Ciocan, G. Ponchak, and S. R. LeClair, "Transient thermography using evanescent microwave microscope," *Rev. Sci. Instrum.*, vol. 70, no. 8, pp. 3387–3390, 1999.

[20] M. Tabib-Azar, J. L. Katz, and L. Clair, "Evanescent microwaves: A novel super-resolution noncontact nondestructive imaging technique for biological applications," *IEEE Trans. Instrum. Meas.*, vol. 48, no. 6, pp. 1111–1116, Dec. 1999.

[21] F. Keilmann, B. Knoll, and A. Kramer, "Long-wave-infrared near-field microscopy," *Phys. Statist. Sol.*, vol. 215, pp. 849–854, 1999.

[22] M. J. Hagmann, P. Andrei, S. Pandey, and A. Nahata, "Possible applications of scanning frequency comb microscopy for carrier profiling in semiconductors," *J. Vac. Sci. Technol.*, vol. 33, no. 2, pp. 02B109-1–02B109-6, 2015.

[23] H. -G. von Ribbeck *et al.*, "Spectroscopic THz near-field microscope," *Opt. Exp.*, vol. 16, no. 5, pp. 3430–38, 2008.

[24] B. Bhushan, ed., *Scanning Probe Microscopy in Nanoscience and Nanotechnology*, vol. 2. Berlin, Germany: Springer, 2011, p. 816.

[25] S. M. Anlage, V. V. Talanov, and A. R. Schwartz, "Principles of near-field microwave microscopy," in *Scanning Probe Microscopy*, S. Kalinin and A. Gruverman, Eds. New York, NY, USA: Springer, 2007, pp. 215–253.

[26] K. T. McDonald, "Radiation from the open end of a coaxial cable," Jun. 25, 2014. Accessed: Jul. 12, 2021. [Online]. Available: https://www.physics.princeton.edu/~mcdonald/examples/coax_rad.pdf

[27] T. M. Wallis and P. Kabos, "Measurement techniques for radio frequency nanoelectronics," in *The Cambridge RF and Microwave Engineering Series*. Cambridge, U.K.: Cambridge Univ. Press, 2017.

[28] H. Tanbakuchi, M. Richter and M. Whitener, "Design of scanning capacitance microscope," in *Proc. 68th ARFTG Conf., Microw. Meas.*, 2006, pp. 1–4.

[29] H. Tanbakuchi, M. Richter, F. Kienberger, and H. Huber, "Nanoscale materials and device characterization via a scanning microwave microscope," *Proc. IEEE Int. Conf. Microw., Commun. Antennas Electron. Syst.*, 2009, pp. 1–4.

[30] P. F. Medina *et al.*, "Transmission and reflection mode scanning microwave microscopy (SMM): Experiments, calibration, and simulations," in *Proc. Eur. Microw. Conf.*, 2015, pp. 654–657.

[31] X. Jin, M. Farina, X. Wang, G. Fabi, X. Cheng and J. C. M. Hwang, "Broadband scanning microwave microscopy of a biological cell with unprecedented image quality and signal-to-noise ratio," in *Proc. IEEE MTT-S Int. Microw. Symp.*, 2019, pp. 216–219.

[32] M. Farina *et al.*, "Disentangling time in a near-field approach to scanning probe microscopy," *Nanoscale*, vol. 3, no. 9, p. 3589–3593, 2011.

[33] B. Rosner and D. W. van der Weide, "High-frequency near-field microscopy," *Rev. Sci. Instrum.*, vol. 75, no 7, pp. 2505–2525, 2002.

[34] A. Imtiaz, T. M. Wallis, and P. Kabos, "Near-field scanning microwave microscopy," *IEEE Microw. Mag.*, vol. 15, no. 1, pp. 52–64, Jan. 2014.

[35] K. Lee, H. Melikyan, A. Babjanyan, and B. Friedman, "Near-field microwave microscopy for nanoscience and nanotechnology," in *Scanning Probe Microscopy in Nanoscience and Nanotechnology*, B. Bhushan, Ed. Berlin, Germany: Springer, 2011, Ch. 5, vol. 2, pp. 135–169.

[36] S. Kalinin and A. Gruverman, Eds., *Scanning Probe Microscopy*. New York, NY, USA: Springer, 2007, p. 980.

[37] J. Kopanski, L. You, J. Ahn, E. Hitz, and Y. Obeng, "Scanning probe microscopes for subsurface imaging," *ECS Trans.*, vol. 61, no. 2, pp. 185–93, 2014.

[38] H. P. Huber *et al.*, "Calibrated nanoscale capacitance measurements using a scanning microwave microscope," *Rev. Sci. Instrum.,* vol. 81, no. 11, pp. 113701–113710, Nov. 2010.

[39] M. Farina, D. Mencarelli, A. Di Donato, G. Venanzoni, and A. Morini, "Calibration protocol for broadband near-field microwave microscopy," *IEEE Trans. Microw. Theory Techn.*, vol. 59, no. 10, pp. 2769–2776, Oct. 2011.

[40] G. Gramse, M. Kasper, L. Fumagalli, G. Gomila, P. Hinterdorfer, and F. Kienberger, "Calibrated complex impedance and permittivity measurements with scanning microwave microscopy," *Nanotechnology*, vol. 25, no. 14, pp. 145703–145711, Apr. 2014.

[41] M. Kasper, G. Gramse and F. Kienberger, "An advanced impedance calibration method for nanoscale microwave imaging at broad frequency range," *IEEE Trans. Microw. Theory Techn.*, vol. 65, no. 7, pp. 2418–2424, Jul. 2017.

[42] G. Fabi *et al.*, "Real-time removal of topographic artifacts in scanning microwave microscopy," *IEEE Trans. Microw. Theory Techn.*, vol. 69, no. 5, pp. 2662–2672, May 2021.

[43] J. Caspermeyer, *ASU Spin-Out Company Acquired by Agilent Technologies*. Tempe, AZ, USA: Arizona State Univ., Dec. 2005. Accessed: Jul. 16, 2021. [Online]. Available: https://biodesign.asu.edu/news/asu-spin-out-company-acquired-agilent-technologies

[44] F. M. Serry, "Scanning microwave microscope mode," Agilent Technologies Application Note 5989-8818EN Rev A, Aug. 2008, p. 4.

[45] Agilent, "Scanning microwave microscopy (SMM) mode: Highly sensitive imaging mode for complex, calibrated electrical and spatial measurements," Agilent Technologies Data Sheet 5989-8817EN, Aug. 26, p. 4, 2008.

[46] S. Tuca, M. Kasper, F. Kienberger and G. Gramse, "Interferometer scanning microwave microscopy: Performance evaluation," *IEEE Trans. Nanotechnol.*, vol. 16, no. 6, pp. 991–998, Nov. 2017.

[47] F. Kienberger, private communication. Jul. 19, 2021.

[48] European Commission, "Microwave nanotechnology for semiconductor and life sciences," Fact Sheet, Record 105567, p. 6, Aug. 2016, Accessed: Jul. 1, 2021. [Online]. Available: https://cordis.europa.eu/project/id/317116

[49] B. Volk, *General Manager, General Letter to Customers*. Santa Clara, CA, USA: Keysight Technologies, Mar. 2018.

[50] Song Xu, "Formerly of keysight technologies," private communication, Jul. 14, 2021.

[51] E. Brinciotti, G. Badino, M. Kasper, and F. Kienberger, "Scanning microwave microscopy for quantitative imaging of biological samples including live cells," Keysight Application Note 5992-1762EN, Aug. 2016, p. 12.

[52] Oxford Instruments Asylum Research, Santa Barbara, CA, USA, 2021. Accessed: Jul. 17, 2021. [Online]. Available: https://afm.oxinst.com/

[53] PrimeNano Inc., Santa Clara, CA, USA, 2021. Accessed: Jul. 17, 2021. [Online]. Available: https://www.primenanoinc.com/

[54] M. Kasper, G. Gramse and F. Kienberger, "An advanced impedance calibration method for nanoscale microwave imaging at broad frequency range," *IEEE Trans. Microw. Theory Techn.*, vol. 65, no. 7, pp. 2418–2424, Jul. 2017.

[55] P.H. Siegel, "THz Pioneers: Fritz Keilmann: RF biophysics: From Strong field to near field," *IEEE Trans. THz Sci. Technol.*, vol. 3, no. 5, pp. 505–514, Sep. 2013. [Online]. Available: https://ethw.org/Archives:THz_and_Microwave_Pioneers

[56] F. Keilmann, "FIR microscopy," *Infrared Phys. Tech*., vol. 36, no. 1, pp. 217–224, 1995.

[57] A. Kramer, F. Keilmann, B. Knoll, and R. Gluckenberger, "The coaxial tip as a nano-antenna for scanning near-field microwave transmission microscopy," *Micron*, vol. 27, no. 6, pp. 413–417, 1996.

[58] B. Knoll, F. Keilmann, and R. Gluckenberger, "Contrast of microwave near-field microscopy," *Appl. Phys. Lett.,* vol. 70, no. 20, pp. 2667–2669, 1997.

[59] B. Knoll and F. Keilmann, "Near-field probing of vibrational absorption for chemical microscopy," *Nature,* vol. 399, pp. 134–137, 1999.

[60] B. Knoll and F. Keilmann, "Infrared conductivity mapping for nanoelectronics" *Appl. Phys. Lett.,* vol. 77, no. 24, pp 3980–82, 2000.

[61] R. Hillenbrand and F. Keilmann, "Complex optical constants on a subwavelength scale," *Phys. Rev. Lett.*, vol. 85, no. 4, pp. 3029–3032, 2000.

[62] F. Keilmann and R. Hillenbrand, "Near-field microscopy by elastic light scattering from a tip," *Phil. Trans. R. Soc. A*, vol. 362, no. 1817, pp. 787–805, 2004.

[63] R. Hillenbrand, B. Knoll, and F. Keilmann, "Pure optical contrast in scattering-type scanning near-field microscopy," *J. Microscopy*, vol. 202, pp. 77–83, 2001.

[64] F. Zenhausern, M. P. Doyle, and H. K. Wickramasinghe, "Apertureless near-field optical microscope," *Appl. Phys. Lett.*, vol. 65, no. 13, pp. 1623–1625, 1994.

[65] T. Wei, X. -D. Xiang, W. G. Wallace-Freedman, and P. G. Schultz, "Scanning tip microwave near-field microscope, "*Appl. Phys. Lett.*, vol. 68, no. 24, pp. 3506–3058, 1996.

[66] H. T. Chen, R. Kersting, and G. C. Cho, "THz imaging with nanometer resolution," *Appl. Phys. Lett.*, vol. 83, no. 15, pp. 3009–3011, 2003.

[67] CENS News, "New company: Neaspec GmbH," Ludwig Maximilians Univ. Archive, Jul. 10, 2007. Accessed: Jul. 20, 2021. [Online]. Available: http://www.cens.de/news/archive/archiv-single/article//new-company/

[68] S. Master *et al.*, "Terahertz nanofocusing with cantilevered terahertz-resonant antenna tips," *Nano Lett.*, vol. 17, no. 11, pp. 6526–6533, 2017.

[69] D. H. Auston and M. C. Nuss, "Electrooptic generation and detection of femtosecond electrical transients," *IEEE J. Quantum Electron.*, vol. 24, no. 2, pp. 184–197, Feb. 1988.

[70] D. Grischkowsky, R. Kesselring, and F. K. Kneubuehl, Eds., "Time-domain, far-infrared spectroscopy," in *Proc. 4th Int. Conf. Infrared Phys.*, 1988, pp. 51–60.

[71] H. von Ribbeck *et al.*, "Spectroscopic THz near-field microscope," *Opt. Exp.,* vol. 16, no. 5, pp. 3430–3438, 2008.

[72] A. Cvitkovic, N. Ocelic and R. Hillenbrand, "Analytical model for quantitative prediction of material contrasts in scattering-type near-field optical microscopy," *Opt. Exp.*, vol. 15, no. 4, pp. 8550–8565, 2007.

[73] A. J. Huber, F. Keilmann, J. Wittborn, J. Aizpurua, and R. Hillenbrand, "Terahertz near-field nanoscopy of mobile carriers in single semiconductor nanodevices," *Nano Lett.*, vol. 8, no. 11, pp. 3766–3770, 2008.

[74] A. Bartels, R. Cerna, C. Kistner, A. Thoma, F. Hudert, C. Janke, and T. Dekorsy, "Ultrafast time-domain spectroscopy based on high-speed asynchronous optical sampling," *Rev. Sci. Instrum.*, vol. 78, pp. 035107-1-035107-8, 2007.

[75] A. Alonso-Gonzalez *et al.*, "Acoustic terahertz graphene plasmons revealed by photocurrent nanoscopy," *Nature Nanotechnol.*, vol. 12, pp. 31–35, 2017.

[76] C. Liewald, S. Mastel, J. Hesler, A. Huber, R. Hillenbrand, and F. Keilmann, "All-electronic terahertz nanoscopy," *Optica*, vol. 5, no. 2, pp. 159–163, 2018.

[77] M. C. Giordano *et al.*, "Phase-resolved terahertz self-detection near-field microscopy," *Opt. Exp.*, vol. 25, no. 14, pp. 18423–18435, 2018.

[78] C. Maissen, S. Chen, E. Nikulina, A. Govyadinov, and R. Hillenbrand, "Probes for ultrasensitive THz nanoscopy," *ACS Photon.,* vol. 6, no. 5, pp. 1279–88, 2019.

[79] N. Aghamiri, F. Huth, A. Huber, A. Fali, R. Hillenbrand, and Y. Abate, "Hyperspectral time-domain terahertz nano-imaging," *Opt. Exp.*, vol. 27, no. 17, pp. 24231–24242, 2019.

[80] C. Chen *et al.*, "Terahertz nanoimaging and nanospectroscopy of chalcogenide phase-change materials," *ACS Photon.*, vol. 7, no. 12, pp. 3499–3506, 2020.

[81] M. Schnell, M. Goikoetxea, I. Amenabar, P. S. Carney, and R. Hillenbrand, "Rapid infrared spectroscopic nanoimaging with nano-FTIR holography," *ACS Photon.*, vol. 7, no. 10, pp. 2878–2885, 2020.

[82] E. Pogna, C. Silvestri, L. Columbo, M. Brambilla, G. Scamarcio, and M. Vitiello, "Terahertz near-field nanoscopy based on detectorless laser feedback interferometry under different feedback regimes," *APL Photon.*, vol. 6, no. 6, pp. 061302 1-9, 2021.

[83] T. de Oliveira *et al.*, "Nanoscale-confined terahertz polaritons in a Van der Waals crystal," *Adv. Mater.*, vol. 33, no 2, pp. 2005777 1-7, 2021.

[84] T. L. Cocker, V. Jelic, R. Hillenbrand, and F.A. Hegmann, "Nanoscale terahertz scanning probe microscopy," *Nature Photon.*, vol. 15, no. 8, pp. 558–569, Aug. 2021.

[85] R. Höber, "Eine methode die elektrische leitfaehigkeit im innern von zellen zu messen," *Arch. Ges. Physiol.*, vol. 133, pp. 237–259, 1910. English translation. [Online]. Available: https://hoebers.wordpress.com/2020/08/27/a-century-old-experiment-still-relevant-today/

[86] M. Philippson, "Les lois de la résistance électrique des tissus vivants," *Bull. Cl. Sci. Acad. R. Belg.*, ser. 5, vol. 7, no. 7, pp. 387–403, Jul. 1921. (English translation). [Online]. Available: http://arxiv.org/abs/2105.06428

[87] C. M. Carpenter and A. B. Page, "Production of fever in man by short radio waves," *Science*, vol. 71, no. 1844, pp. 450–452, 1930.

[88] P. H. Siegel, "Microwaves are everywhere: Ovens, from magnetrons to metamaterials," *IEEE J. Microwaves*, vol. 1, no. 2, pp. 523–531, Apr. 2021.

[89] G. H. Haggis, T. J. Buchanan, and J. B. Hasted, "Estimation of the protein hydration by dielectric measurements at microwave frequencies," *Nature*, vol. 167, no. 4250, pp. 607–608, 1951.

[90] W. von Casimir, N. Kaiser, F. Keilmann, A. Mayer, and H. Vogel, "Dielectric properties of oxyhemoglobin and deoxyhemoglobin in aqueous solution at microwave frequencies," *Biopolymers,* vol. 6, no. 12, pp. 1705–1715, 1968.

[91] Y. Wang and M. Tabib-Azar, "Microfabricated near-field scanning microwave probes," in *Dig. Int. Electron Devices Meeting*, 2002, pp. 905–907.

[92] M. Tabib-Azar and Y. Wang, "Design and fabrication of scanning near-field microwave probes compatible with atomic force microscopy to image embedded nanostructures," *IEEE Trans. Microw. Theory Techn.*, vol. 52, no. 3, pp. 971–979, Mar. 2004.
[93] J. Park, S. Hyun, A. Kim, T. Kim, and K. Char, "Observation of biological samples using a scanning microwave microscope," *Ultramicroscopy*, vol. 102, no. 2, pp. 101–106, Jan. 2005.
[94] K. Lai, M. B. Ji, N. Leindecker, M. A. Kelly, and Z. X. Shen, "Atomic force-microscope-compatible near-field scanning microwave microscope with separated excitation and sensing probes," *Rev. Sci. Instrum.*, vol. 78, no. 6, Jun. 2007, Art. no. 063702.
[95] A. N. Reznik and N. V. Yurasova, "Electrodynamics of microwave near-field probing: Application to medical diagnostics," *J. Appl. Phys.*, vol. 98, no. 11, pp. 114701-1–114701-9, 2005.
[96] M. Brehm, T. Taubner, R. Hillenbrand, and F. Keilmann, "Infrared spectroscopic mapping of single nanoparticles and viruses at nanoscale resolution," *Nano Lett.*, vol. 6, no. 7, pp. 1307–1310, 2006.
[97] E. Bründermann, D. A. Schmidt, I. Kopf, K. Meister, M. Filimon, and M. Havenith, "Chemical microscopy and nanoscopy of bio-materials and living cells," in *Proc. 35th Int. Conf. Infrared Millimeter THz Waves*, 2010, pp. 1–2.
[98] F. Ballout *et al.*, "Scanning near-field IR microscopy of proteins in lipid bilayers," *Phys. Chem. Chem. Phys.*, vol. 13, no. 48, pp. 21432–36, 2011.
[99] I. Amenabar *et al.*, "Structural analysis and mapping of individual protein complexes by infrared nanospectroscopy," *Nature Comm.,* vol. 4, no. 2890, pp. 1–9, 2013.
[100] F. Huth, M. Schnell, J. Wittborn, N. Ocelic, and R. Hillenbrand, "Infrared spectroscopic nanoimaging with a thermal source," *Nature Mater.*, vol. 10, no. 5, pp. 352–6, 2011.
[101] K. Kaltenecker, T. Goelz, E. Bau, and F. Keilmann, "Infrared-spectroscopic near-field microscopy of living cells and nanoparticles in water," submitted to: *Scientific Reports*, Aug. 2021.
[102] Z. Li *et al.*, "Single cell imaging with near-field terahertz scanning Microscopy," *Cell Proliferation*, vol. 53, no. 4, pp. 1–7, 2020.
[103] Y. J. Oh *et al.*, "High-frequency electromagnetic dynamics properties of THP1 cells using scanning microwave microscopy," *Ultramicroscopy*, vol. 111, no. 11, pp. 1625–1629, Nov. 2011.
[104] S. -S. Tuca *et al.*, "Calibrated complex impedance of CHO cells and E. coli bacteria at GHz frequencies using scanning microwave microscopy," *Nanotechnology*, vol. 27, no. 13, Apr. 2016, Art. no. 135702.
[105] M. C. Biagi *et al.*, "Nanoscale electric permittivity of single bacterial cells at gigahertz frequencies by scanning microwave microscopy," *ACS Nano*, vol. 10, no. 1, pp. 280–288, 2016.
[106] E. Brinciotti *et al.*, "Scanning microwave microscopy for quantitative imaging of biological samples including live cells," Keysight Technologies Application Note, 5992-1762EN, p. 12, Aug. 30, 2016.
[107] G. Gramse, A. Schönhais, and F. Kienberger, "Nanoscale dipole dynamics of protein membranes studied by broadband dielectric microscopy," *Nanoscale*, vol. 11, no. 10, pp. 4303–4309, 2019.
[108] S. Grall *et al.*, "Attoampere nanoelectrochemistry," *Small*, vol. 17, no. 29, pp. 2101253-1-2101253-7, 2021.
[109] M. Farina and J. C. M. Hwang, "Scanning microwave microscopy for biological applications," *IEEE Microw. Mag*., vol. 21, no. 10, pp. 52–59, Oct. 2020.
[110] M. Farina, A. Di Donato, D. Mencarelli, G. Venanzoni, and A. Morini, "High resolution scanning microwave microscopy for applications in liquid environment," *IEEE Microw. Wireless Compon. Lett.*, vol. 22, no. 11, pp. 595–597, Nov. 2012.
[111] T. D. Pham, P. Q. Pham, J. Li, A. G. Letai, D. C. Wallace, and P. J. Burke, "Cristae remodeling causes acidification detected by integrated graphene sensor during mitochondrial outer membrane permeabilization," *Sci. Rep.*, vol. 6, no. 1, Dec. 2016, Art. no. 35907.
[112] J. Li, Z. Nemati, K. Haddadi, D. C. Wallace, and P. J. Burke, "Scanning microwave microscopy of vital mitochondria in respiration buffer," in *IEEE MTT-S Int. Microw. Symp. Dig*., Jun. 2018, pp. 115–118.
[113] Z. Nemati, J. Li, and P. J. Burke, "Integrated fluorescence and scanning microwave microscopy: Nano-imaging with 'proof of life'," in *Proc. IEEE Radio Antenna Days Indian Ocean*, 2019, pp. 1–2.
[114] M. Farina *et al.*, "Investigation of fullerene exposure of breast cancer cells by time-gated scanning microwave microscopy," *IEEE Trans. Microw. Theory Techn.*, vol. 64, no. 12, pp. 4823–4831, Dec. 2016.
[115] X. Jin *et al.*, "Imaging of exosomes by broadband scanning microwave microscopy," in *Proc. 46th Eur. Microw. Conf.,* 2016, pp. 1211–1214.
[116] X. Jin, M. Farina, X. Wang, G. Fabi, X. Cheng, and J. C. M. Hwang, "Quantitative scanning microwave microscopy of the evolution of a live biological cell in a physiological buffer," *IEEE Trans. Microw. Theory Techn.*, vol. 67, no. 12, pp. 5438–5445, Dec. 2019.
[117] M. Farina *et al.*, "Inverted scanning microwave microscope for *in vitro* imaging and characterization of biological cells," *Appl. Phys. Lett.*, vol. 114, no. 9, pp. 093703-1–093703-3, plus Suppl. Mater., 2019.
[118] G. Fabi *et al.*, "Electrical properties of Jurkat cells: An inverted scanning microwave microscope study," in *Proc. IEEE/MTT-S Int. Microw. Symp.*, 2020, pp. 237–240.
[119] G. Fabi *et al.*, "Quantitative characterization of platinum diselenide electrical conductivity with an inverted scanning microwave microscope," *IEEE Trans. Microw. Theory Techn.*, vol. 69, no. 7, pp. 3348–3359, Jul. 2021.
[120] A. Tselev, J. Velmurugan, A. V. Ievlev, S. V. Kalinin, and A. Kolmakov, "Seeing through walls at the nanoscale: Microwave microscopy of enclosed objects and processes in liquids," *ACS Nano*, vol. 10, no. 3, pp. 3562–3570, Mar. 22, 2016.
[121] A. Tselev, "Near-field microwave microscopy: Subsurface imaging for in situ characterization," *IEEE Microw. Mag.*, vol. 21, no. 10, pp. 72–86, Oct. 2020.
[122] L. Fumagalli, *et al.*, "Anomalously low dielectric constant of confined water," *Science,* vol. 360, no. 6395, pp. 1339–1342, 2018.
[123] P. H. Siegel, "Microwaves are everywhere, CMB: Hiding in plain sight," *IEEE J. Microwaves*, vol. 1, no. 1, pp. 14–24, Jan. 2021.

PETER H. SIEGEL (Life Fellow, IEEE) received the B.A. degree in astronomy from Colgate University, Hamilton, NY, USA, in 1976, the M.S. degree in physics and the Ph.D. degree in electrical engineering from Columbia University, New York City, NY, USA, in 1978 and 1983, respectively. He has held appointments as a Research Fellow and Engineering Staff with the NASA Goddard Institute for Space Studies, New York City, NY, USA, from 1975 to 1983, a Staff Scientist with the National Radio Astronomy Observatory, Central Development Labs, Charlottesville, VA, USA, from 1984 to 1986, a Technical Group Supervisor and Senior Research Scientist with the Jet Propulsion Laboratory (JPL), National Aeronautics and Space Administration (NASA), Pasadena, CA, USA, from 1987 to 2014, and a Faculty Associate in electrical engineering and Senior Scientist in biology with the California Institute of Technology (Caltech), Pasadena, CA, USA, from 2002 to 2014. With JPL, he founded and led for 25 years, the Submillimeter Wave Advanced Technology Team, a group of more than 20 scientists and engineers developing THz technology for NASA's near and long-term space missions. These included delivering key components for four major satellite missions and leading more than 75 smaller research and development programs for NASA and the U.S. Department of Defense. With Caltech, he was involved in new biological and medical applications of THz, especially low-power effects on neurons and most recently millimeter-wave monitoring of blood chemistry. He was an IEEE Distinguished Lecturer and the Vice-Chair and Chair of the IEEE MTTS THz Technology Committee. He is currently an elected Member of the MTTS AdCom. He has more than 300 articles on THz components and technology and has given more than 250 invited talks on this subject throughout his career of 45 years in THz. His current appointments include the CEO of THz Global, a small research and development company specializing in RF bio-applications, a Senior Scientist Emeritus of biology and electrical engineering with Caltech, and a Senior Research Scientist Emeritus and a Principal Engineer with the NASA Jet Propulsion Laboratory. He was recognized with 75 NASA Technology awards, ten NASA team awards, the NASA Space Act Award, three individual JPL awards for technical excellence, four JPL team awards, and the IEEE MTTS Applications Award in 2018. He is honored to take up the responsibility as the Founding Editor-in-Chief of IEEE JOURNAL OF MICROWAVES, which he hopes will invigorate the microwave field. Among many other functions, he was the Founding Editor-in-Chief of IEEE TRANSACTIONS ON TERAHERTZ SCIENCE AND TECHNOLOGY, from 2010 to 2015, and the Founder, in 2009, Chair through 2011, and elected General Secretary since 2012, of the International Society of Infrared, Millimeter, and Terahertz Waves, the world's largest society devoted exclusively to THz science and technology.